sensors

MDPI

Article

Nonlinear Frequency Offset Beam Design for FDA-MIMO Radar

Yanjie Xu, Chunyang Wang, Guimei Zheng * and Ming Tan

College of Air and Missile Defense, Air Force Engineering University, Xi'an 710051, China
* Correspondence: zheng-gm@163.com

Abstract: The beam pattern of frequency diversity array (FDA) radar has a range–angle two-dimensional degree of freedom, which makes it possible to distinguish different targets from the same angle and brings a new approach to anti-jamming of radars. However, the beam pattern of conventional linearly frequency-biased FDA radar is range–angle-coupled and time-varying. The method of adding nonlinear frequency bias among the array elements of the FDA array has been shown to eliminate this coupling property while still allowing for better beam performance of the emitted beam. In this paper, we obtain a decoupled and time-invariant beam direction map using the FDA-multi-input–multi-output (FDA-MIMO) radar scheme and then obtain a sharp pencil-shaped main sphere beam pattern with range–angle dependence using a linear frequency offset scheme weighted by a Chebyshev window. Finally, the anti-interference performance of the proposed method is verified in an anti-interference experiment.

Keywords: nonlinear frequency offset; FDA-MIMO radar; Chebyshev window based frequency offset; array structure design

check for updates

Citation: Xu, Y.; Wang, C.; Zheng, G.; Tan, M. Nonlinear Frequency Offset Beam Design for FDA-MIMO Radar. *Sensors* **2023**, *23*, 1476. https://doi.org/10.3390/s23031476

Academic Editors: Jianfeng Li and Ding Wang

Received: 3 December 2022
Revised: 27 December 2022
Accepted: 4 January 2023
Published: 28 January 2023

Copyright: © 2023 by the authors. Licensee MDPI, Basel, Switzerland. This article is an open access article distributed under the terms and conditions of the Creative Commons Attribution (CC BY) license (https://creativecommons.org/licenses/by/4.0/).

1. Introduction

Since the first introduction of FDA radars in [1], the important property that their beam patterns are range-dimension dependent and can vary with time has been discovered, which has attracted extensive attention from scholars home and abroad. When the time and frequency offsets are fixed, the emission direction pattern of the frequency-controlled array has a range–angle-dependent property, which is more flexible compared with the conventional phased array and has a very high potential in practical applications [2–6]. However, the conventional fixed-frequency offsets FDA emission direction diagram is "S" shaped, with range–angle coupling characteristics, and is time-varying, which is unfavorable for the practical application of radar. With the exploration of the nature of the FDA directional pattern characteristics, many beam design methods for FDA radars have emerged. The range–angle coupling characteristics of FDA radar is caused by introducing the frequency offset among the array elements, so the frequency offset also needs to be designed and optimized to solve the coupling problem. The first problem to be solved is the time-varying problem. The literature [7] studied the time-varying problem of FDA radar and designed a time-invariant beam pattern, and the literature [8,9] combined FDA radar with MIMO technology to form a time-invariant beam pattern as well. On the basis of the existing research, the literature [10] explored the fundamental reason for the time-varying nature of the beam pattern from the nature of FDA radar and proposed the concept of "time figure", which is of guidance for FDA radar research. After a period of research, the FDA-MIMO radar regime was proved to be one of the available methods to solve the beam patterns' coupling problems [11,12]. After solving the time-varying problem, the beam performance is the next issue to be considered. On the basis of ensuring the time invariance, many beam design schemes have been proposed to provide a more superior performance. A logarithmic frequency offset scheme is proposed in the literature [13], which solves

the periodic problem in space and forms a point beam, but with poor performance. The literature [14] uses a particle swarm optimization algorithm to determine the frequency offsets and array element spacing to form a point-like transmit beam map, which also has a lower side flap in the range dimension, but the calculation is too complex. As studies proceeded, the design of FDA radar frequency offsets using a window function weighting scheme became popular. However, window function weighting schemes based on fixed windows have been studied more often, while window function weighting schemes based on flexible windows are still less mentioned [14–22]. Compared with the fixed window function, the flexible window function can have more degrees of freedom in the power proportion of the main and side flaps, and, therefore, a better performance of the beam direction map can be obtained [23]. Overall, the present research on frequency-controlled array transmit beam formation can basically solve the problems of coupling and periodicity, but the present beam design scheme still has the problems of insufficient beam main flap focus, low beam resolution, and high side flap, which is more unfavorable for the specific application of radar. Therefore, it is necessary to design a point-type transmitting beam with narrow main flap and low side flap. For linear frequency bias, the beam direction map is not point-like, which is not favorable for radar detection, and because of this, a frequency bias design is needed to improve the beam direction map performance. In this paper, the time-invariant FDA beam direction diagram is obtained on the basis of the FDA-MIMO radar system, and the beam is further optimized by using the Chebyshev window to weight the linear frequency offsets on the basis of the existing nonlinear frequency offsets schemes, obtaining the results of narrowing the main flap and reducing the side flaps of the transmit beam. To better test its application capability, it is combined with the Minimum Variance Distortion-free Response (MVDR) adaptive beamforming algorithm to test its performance in jamming immunity. The simulation results show that this scheme has a more obvious advantage in the beam pattern performance compared with several window function weighted frequency offset schemes that have been proposed.

2. System Model

From the literature [10], we know that an effective measure to eliminate the time parameter in the transmit–receive diagram is to use a series of mixers and matched filters at the receiver. Analogously to this case, we can also use a combination of FDA-MIMO radar and multiple matched filters at the receiver side to produce beam maps independent of the time parameters. Consider a narrow-band FDA-MIMO radar system with M transmitting and N receiving arrays, and design both transmitting and receiving arrays as conventional linear arrays. Suppose the range between transmitting arrays is d_T, the range between receiving arrays is d_R, and the signal carrier frequency is f_0; such a system configuration is shown in Figure 1.

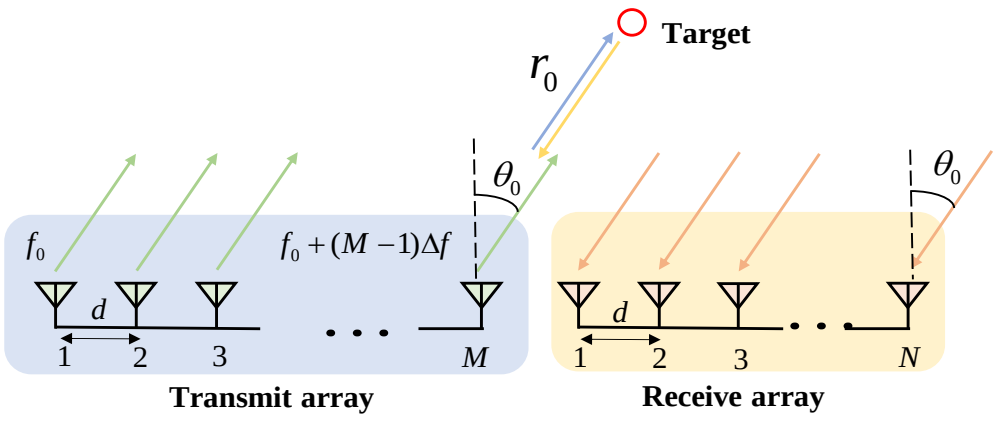


Figure 1. FDA-MIMO Radar System.

As shown in the figure, the frequency offset of the mth element is $f(m)$, and the emission frequency of the mth array element can be expressed as

$$f_m = f_0 + f(m) \tag{1}$$

Suppose each array element emits the same waveform, then the signal emitted by the mth array element at time t can be expressed as Equation (2)

$$s_m(t) = w_m(t)e^{j2\pi f_m t} \tag{2}$$

where $w_m(t)$ is the orthogonal signal envelope emitted by the mth array element, which satisfies

$$\int {w_{m1}}^*(t) \cdot w_{m2}(t-\tau)dt = 0, m1 \neq m2. \tag{3}$$

where ${w_{m1}}^*(t)$ is the conjugate of the $w_{m1}(t)$. With the FDA-MIMO regime radar, the time delay at the target can be expressed as

$$\tau_{m,n} = 2r_0/c - md_T \sin\theta_0/c - nd_R \sin\theta_0/c \tag{4}$$

Then, the received signal related to the mth transmitting array element and the nth receiving array element can be expressed as

$$s_{m,n}(t-\tau_{m,n}) = w_n(t-\tau_{m,n})e^{j\Phi_m(t-\tau_{m,n})} \cdot e^{j2\pi(f_0+f(m))(t-\tau_{m,n})} \tag{5}$$

where $n = 1, 2, \ldots, N$, Φ_m is the phase modulation corresponding to the mth transmitting array element in the FDA-MIMO radar, and the time index can be expressed as

$$t' = t - \frac{2r}{c} \tag{6}$$

Then, under the far-field condition, Equation (2) can be rewritten as

$$s_{m,n}(t') = w_m(t')e^{j\Phi_m(t')}e^{j\varphi_n(t')} \tag{7}$$

In order to eliminate the effect of the time parameter and produce a time-invariant and decoupled transmit beam pattern, we need to use a multi-matching filter approach to process the signal at the receiver side of the FDA-MIMO radar, as shown in Figure 2.

As shown in the figure, the received signal needs to be mixed with the radio frequency of the mixer and later mixed with $w_n(t')$ in the digital signal processor, so that the relative outputs of the mth transmitting array element and the nth receiving array element can be expressed as

$$s_{m,n}^{\text{Output}}(t') = \xi_s e^{j\Phi_m(t')}e^{j\varphi_n(t')} \tag{8}$$

where $\varphi_n(t')$ can be expressed as

$$\begin{aligned} \varphi_n(t') &= 2\pi \int_0^{t'+((md_T\sin\theta/c)+(nd_R\sin\theta/c))} (f_0 + f(m))dx \\ &= 2\pi\left((f_0 + f(m))t' + f_0\frac{md_T\sin\theta}{c} + f_0\frac{nd_R\sin\theta}{c}\right) \end{aligned} \tag{9}$$

If the radar is aimed at the target at (r_t, θ_t), the array factor AF can be expressed as

$$\begin{aligned} AF = &\sum_{m=1}^{M}\sum_{n=1}^{N} s_{m,n}^{\text{output}}(t') = \xi_s e^{-j2\pi f_0((2r/c)+md_T(\sin\theta-\sin\theta_t)/c)} \\ &\cdot \sum_{m=1}^{M} e^{j(4\pi/c)f(m)(r_t-r)} \sum_{n=1}^{N} e^{j(2\pi f_0 nd_R(\sin\theta-\sin\theta_t)/c)} \end{aligned} \tag{10}$$

The transmit–receive normalized beam pattern can be expressed as

$$B = B_T \cdot B_R = \left| \sum_{m=1}^{M} e^{j(4\pi/c)f(m)(r_t - r)} e^{j(2\pi f_0 m d_T(\sin\theta - \sin\theta_t)/c)} \right|^2 \cdot \left| \sum_{n=1}^{N} e^{j(2\pi f_0 n d_R(\sin\theta - \sin\theta_t)/c)} \right|^2 \quad (11)$$

It is worth noting that the transmit–receive beam pattern in the above formula can be equivalent to the multiplication of the transmit beam pattern and the receive beam pattern at the receiver, which can be represented by B_T and B_R, respectively.

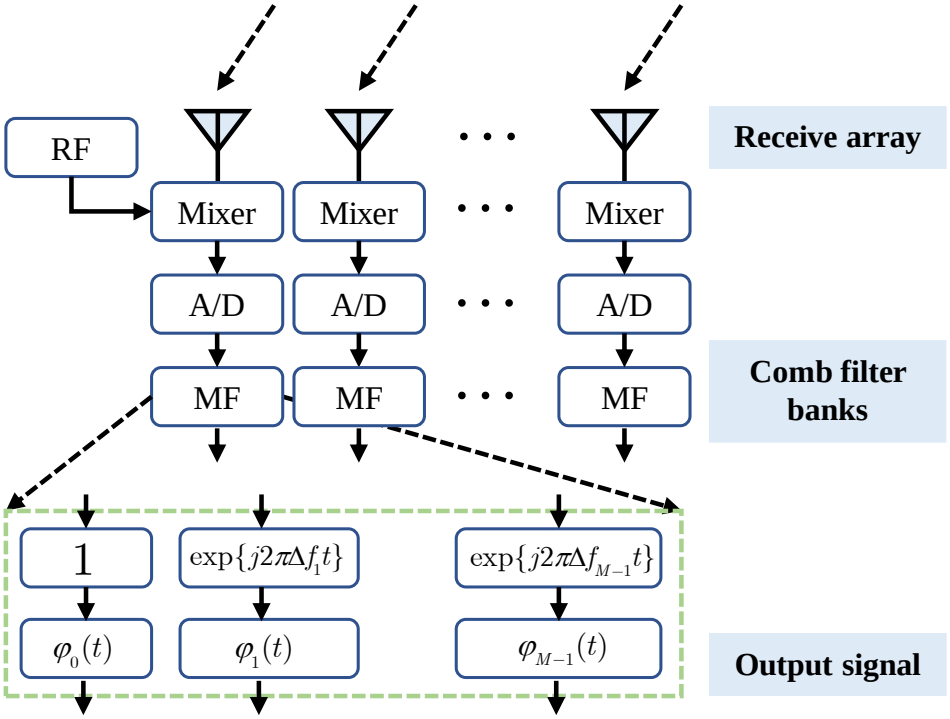


Figure 2. FDA-MIMO and multi-matching filter system.

Equation (11) shows that the FDA-MIMO radar can rely on its own characteristics to produce a time-invariant range-dependent beam pattern after the signal processing process, and that the beam pattern can be maximized at the target point with a maximum value of M^2N^2, regardless of the frequency offset change. Therefore, when designing the beam direction map of the FDA-MIMO radar, the range dependence of the FDA-MIMO radar should be activated by adding the corresponding variables of phase and target spatial position at the transmitter side.

3. Chebyshev Window Weighted Linear Frequency Offsets

For the window function weighted frequency offsets scheme, the parameter selection of the window function is an important element affecting the beam performance. Most of the window functions of variable windows are controlled by two parameters, so it is necessary to use the control variable method to find the best combination of parameters. Ordinarily, when choosing the best position for the performance of a parameter, it is not possible to make both the main flap width and the side flap height optimal. For example, when we set the parameter of the peak side flap of the Chebyshev window to a low level, we can ensure that the side flap energy is low, but the energy will be concentrated in the main flap, resulting in a wide main flap, which we do not expect. When we are designing a beam, we usually give priority to minimizing the width of the main flap if the flap level does not seriously affect the detection. On this basis, the Chebyshev window is utilized for frequency offset design in this paper. The advantage of the Chebyshev window function is that the main flap width of the Chebyshev window is minimum for a given flap height, and

all flaps have the same amplitude, so that the beam with minimum main flap width can be obtained by controlling the flaps within an acceptable range when choosing parameters. For nonlinear frequency offset, the proposed frequency offset methods are: log frequency offset, Hamming window based frequency offset (Ham-FDA), and sinusoidal-weighted frequency offset. Our proposed method is a weighted linear frequency offset based on the Chebyshev window, which outperforms the conventional method in both the main flap width and the side flap height. The Log-FDA frequency offset can be expressed as

$$\Delta f_m^{\log} = \delta \cdot \log(m+1) \tag{12}$$

where δ is a constant, and Δf_m represents the frequency offset of the first transmitting array element. Similarly, the frequency offset of Ham-FDA can be expressed as

$$\Delta f_m^{\mathrm{Ham}} = B\left\{0.54 - 0.46\cos\left[\frac{2\pi(m-(M+1)/2)}{M}\right]\right\} \tag{13}$$

where B is the bandwidth and requires that the number of array elements M should be odd.

The frequency shift of the Hamming window weighted linear frequency offsets (HL-FDA) scheme proposed in the literature [17] can be expressed as

$$\Delta f_m^{HL} = m\Delta f\left\{0.54 - 0.46\cos\left[\frac{2\pi(m-(M+1)/2)}{M}\right]\right\} \tag{14}$$

The frequency offset of the proposed algorithm in this paper can be expressed as

$$\Delta f_m^{proposed} = m\Delta f w_c(m) \tag{15}$$

where $w_{\mathrm{c}}(m)$ is the time domain expression for the Chebyshev window function, which can be expressed as [24]

$$w_{\mathrm{c}}(m) = \frac{\sum_{m=-N}^{S} W_{\mathrm{c}}^0(n)\cos\left(\frac{2\pi}{N}mn\right)}{\sum_{m=-N}^{S} W_{\mathrm{c}}^0(n)} \tag{16}$$

where $W_{\mathrm{c}}^0(n)$ is the discrete spectral expression of the Chebyshev window, and S should be defined as $S = (M-1)/2$. Similarly, there are $s = (m-1)/2$. As with the Hamming window weighting scheme, it is also required here that the number of array elements M should be odd. The algorithm proposed in this paper can be seen in the form of a Chebyshev window combined with a linear array of arrays, where the output signal associated with the mth transmitting array element and the nth receiving array element after processing at the receiver side of the FDA-MIMO system, as shown in Equation (17). The array factor AF can be expressed as Equation (18).

$$\begin{aligned} s_{m,n}^{Output}(t') &\approx rect(\tfrac{t'}{T_p})\xi_s \exp\{j2\pi[-f_0\tfrac{2r}{c} - m\Delta f w_c(m))\tfrac{2r}{c} \\ &+ f_0\tfrac{md_T\sin\theta}{c} + f_0\tfrac{nd_R\sin\theta}{c}]\Big\} \\ &= rect(\tfrac{t'}{T_p})\xi_s \exp\Big\{j2\pi[-f_0\tfrac{2r}{c} - m\Delta f\tfrac{\sum_{m=-N}^{N} W_{\mathrm{c}}^0(n)\cos\left(\frac{2\pi}{N}mn\right)}{\sum_{m=-N}^{N} W_{\mathrm{c}}^0(n)})\tfrac{2r}{c} \\ &+ f_0\tfrac{nd_T\sin\theta}{c} + f_0\tfrac{md_R\sin\theta}{c}]\Big\} \end{aligned} \tag{17}$$

$$\begin{aligned} AF &= \sum_{m=0}^{M-1}\sum_{n=0}^{2N_1} s_{m,n}^{Output}(t') \\ &= rect(\tfrac{t'}{T_p})\xi_s \sum_{m=0}^{M-1}\sum_{n=0}^{2N_1} e^{j2\pi[-f_0\frac{2r}{c} - m\Delta f w_c(m))\frac{2r}{c} + f_0\frac{md_T\sin\theta}{c} + f_0\frac{nd_R\sin\theta}{c}]} \end{aligned} \tag{18}$$

The vector of orientation **A** can be expressed as Equation (19), where **a** and **b** are the transmitting and receiving guide vectors, respectively, which can be expressed as Equations (20) and (21).

$$\mathbf{A} = \xi_s \, \mathbf{a}(r,\theta) \otimes \mathbf{b}(\theta) \tag{19}$$

$$\mathbf{a}(r,\theta) = \begin{bmatrix} 1 \\ e^{j2\pi[f_0 \frac{d_T \sin\theta}{c} - m(\Delta f w_c(m))\frac{2r}{c}]} \\ \vdots \\ e^{j2\pi[f_0 \frac{2Md_T sin\theta}{c} - 2M(\Delta f w_c(m))\frac{2r}{c}]} \end{bmatrix} \tag{20}$$

$$\mathbf{b}(\theta) = \begin{bmatrix} 1 \\ e^{j2\pi f_0 d_R \sin\theta / c} \\ \vdots \\ e^{j2\pi f_0 d_R (N-1) \sin\theta / c} \end{bmatrix} \tag{21}$$

Then, the emission direction diagram $B_{T,R}$ can be expressed as

$$\begin{aligned} B_{T,R} &= \left|\mathbf{w}_D{}^{\mathrm{H}} \cdot \mathbf{A}\right|^2 \\ &= \left|\sum_{n=0}^{2M} \exp\{j2\pi(f_0 d_T m \tfrac{\sin\theta - \sin\theta_0}{c} - 2m\Delta f w_c(m))\}\right|^2 \\ &\times \left|\sum_{n=0}^{N-1} \exp\{j2\pi f_0 d_R n \tfrac{\sin\theta - \sin\theta_0}{c}\}\right|^2 \end{aligned} \tag{22}$$

4. MVDR Algorithm Model

In order to better test the practical application capability of the proposed frequency offsets scheme, it is combined with the adaptive beamforming algorithm to verify its beam output performance under the conventional MVDR algorithm. Adaptive beamforming is an important method to enhance the signal output signal-to-noise ratio in the array radar signal processing process. By attaching a weighting factor between each array element, it causes the array output power to be maximum in the desired direction and minimum in the jamming direction, by which the output signal-to-noise ratio can converge quickly at the jamming location, thus forming a zero null.

In the FDA-MIMO system, the desired signal, the dummy target, and the noise are statistically independent of each other, and the location of the desired target in the setup space is (r_0, θ_0), The interfering signal is i_j, j is the number of jammings, jamming position can be set to (r_j, θ_j), and noise $n(t)$ is Gaussian white noise. The signal at the kth snap count can be expressed as Equation (23), and the output signal in the FDA-MIMO system can be expressed as Equation (24).

$$\boldsymbol{x}(t) = \boldsymbol{a}(r_0,\theta_0)s(t) + \sum_{j=1}^{J} \boldsymbol{a}\big(r_j,\theta_j\big)i_j(t) + \boldsymbol{n}(t) \tag{23}$$

$$\boldsymbol{y}(t) = \boldsymbol{w}^H[\boldsymbol{a}(r_0,\theta_0) \otimes \boldsymbol{b}(\theta_0)]s(t) + \boldsymbol{w}^H \sum_{j=1}^{J} \big[\boldsymbol{a}_0\big(r_j,\theta_j\big) \otimes \boldsymbol{b}_n\big(\theta_j\big)\big] i_j(t) + \boldsymbol{n}(t) \tag{24}$$

To keep the energy of the noise minimum while satisfying the constraints, the optimization function of MVDR can be expressed as

$$\begin{aligned} &\min_{\omega} \mathbf{w}^H \mathbf{R} \mathbf{w} \\ &\text{s.t.} \begin{cases} \mathbf{w}^H \mathbf{a}(r_0,\theta_0) = 1 \\ \mathbf{w}^H \mathbf{a}\big(r_j,\theta_j\big) = 0 \end{cases} \end{aligned} \tag{25}$$

where R is the jamming-plus-noise covariance matrix. The equation can be solved by the Lagrange multiplier method, the optimal weights of the array are obtained as Equation (26), and the output signal-to-jamming-noise ratio (SINR) can be expressed as Equation (27)

$$w_{MVDR} = \frac{\mathbf{R}^{-1}\mathbf{a}(r_0,\theta_0)}{\mathbf{a}(r_0,\theta_0)^H\mathbf{R}^{-1}\mathbf{a}(r_0,\theta_0)} \tag{26}$$

$$R_{SINR} = \frac{\left|\boldsymbol{w}^H\mathbf{a}(r_0,\theta_0)\right|^2}{\boldsymbol{w}^H\boldsymbol{R}^{-1}\boldsymbol{w} - \left|\boldsymbol{w}^H\mathbf{a}(r_0,\theta_0)\right|^2} \tag{27}$$

Finally, incorporating the guidance vector into the above equation, we obtain

$$R_{SINR} = \frac{\left|\boldsymbol{w}^H\left(1, e^{j2\pi[f_0\frac{d_T\sin\theta}{c} - m(\Delta f w_c(m))\frac{2r}{c}]}, \ldots, e^{j2\pi[f_0\frac{2Md_T\sin\theta}{c} - 2M(\Delta f w_c(m))\frac{2r}{c}]}\right)\right|^2}{\boldsymbol{w}^H\boldsymbol{R}^{-1}\boldsymbol{w} - \left|\boldsymbol{w}^H\left(1, e^{j2\pi[f_0\frac{d_T\sin\theta}{c} - m(\Delta f w_c(m))\frac{2r}{c}]}, \ldots, e^{j2\pi[f_0\frac{2Md_T\sin\theta}{c} - 2M(\Delta f w_c(m))\frac{2r}{c}]}\right)\right|^2} \tag{28}$$

5. Simulation and Analysis

5.1. Simulation of Frequency Offset Scheme

In our given FDA-MIMO system, the frequency offset affects only the equivalent transmit beammap and does not affect the receive beammap. Therefore, the simulation compares only the equivalent transmit beamplot. In this section, we simulate and compare the performance of Log-FDA, Ham-FDA, HL-FDA, and our proposed FDA frequency offset scheme. The maximum frequency offsets of these methods are set to be approximately equal, and the other relevant parameters are set as follows. The carrier frequency f_0 is 10 GHz, the array element index is $M = N = 15$, the array spacing of the transmitting and receiving arrays is set to $dt = dr = 0.015$ m, bandwidth is set to $B = 27.5$ kHz, and the target position is set to $(100\text{ km}, 20^\circ)$. Figure 3 compares the array element order versus position for each method.

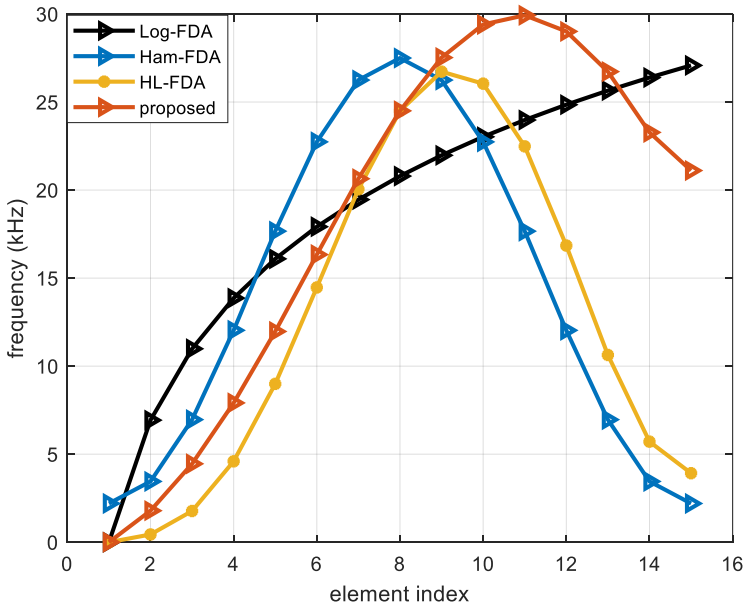


Figure 3. Relationship between array element index and position.

After designing the frequency offset on the FDA-MIMO system, we analyzed the equivalent transmit beamplots of four frequency offset schemes: Log-FDA, Ham-FDA, HL-FDA, and our proposed scheme, as shown in Figure 4.

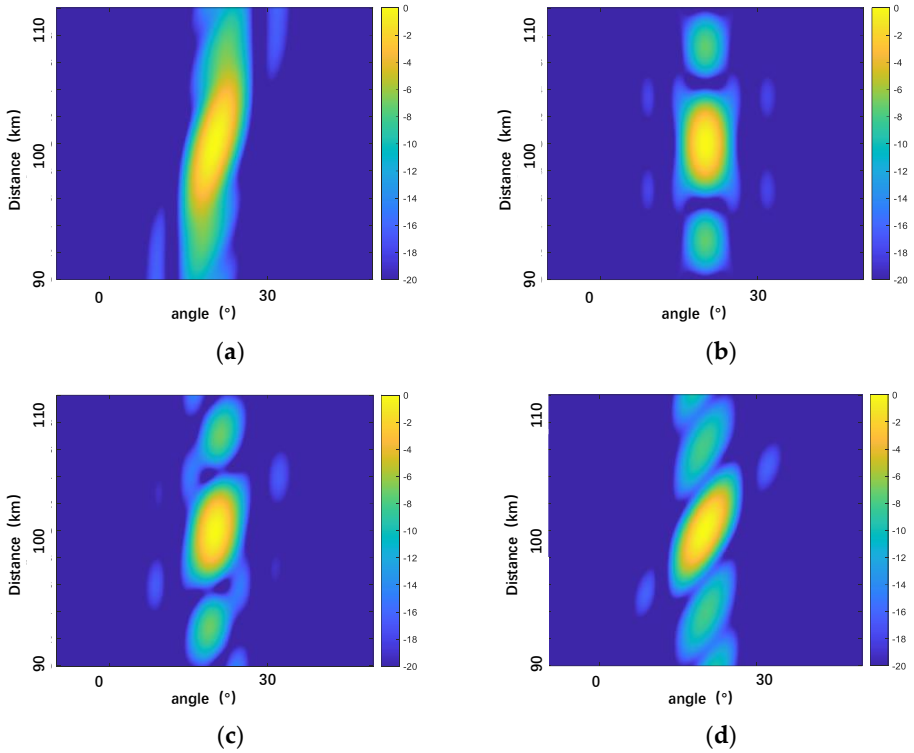


Figure 4. Equivalent transmitting antenna beams of the four schemes: (**a**) Log-FDA; (**b**) Ham-FDA; (**c**) HL-FDA; and (**d**) Proposed.

As shown in Figure 4, several frequency offsets schemes have been proposed to solve the time-varying and coupling problems of the FDA directional map, but the beam performance varies. The Log-FDA scheme can solve the range–angle coupling problem, but the main flap of its formed beam is too wide and does not focus well, and the Ham-FDA and HL-FDA schemes can focus the emitted energy at a point in space. The Ham-FDA and HL-FDA schemes can produce a point-like beam, but the main flap of these two schemes is still very wide, and their side flaps are high in height, which also affects the radar detection performance to some extent. Our proposed method can produce a more focused point-like beam with a lower side flap than the other methods. The 3D view of the beam provides a more intuitive view of the overall effect of the beam, which is shown in Figure 5.

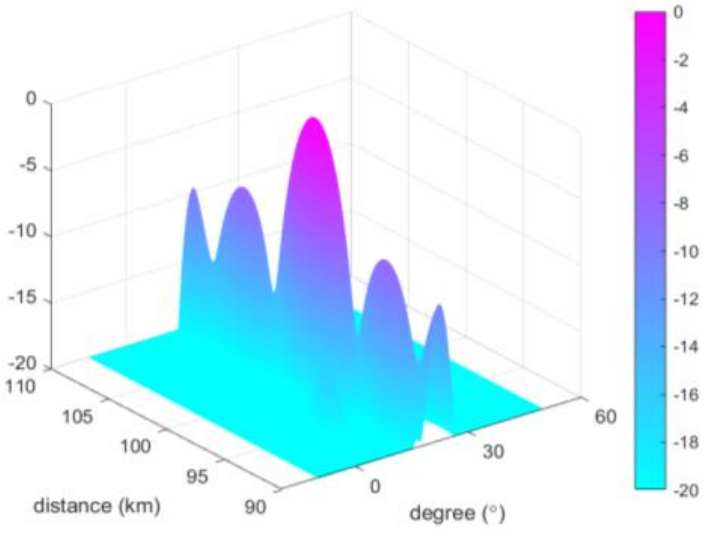


Figure 5. The 3D beam pattern.

As shown in Figure 5, it can be seen that our designed beam produces a lower side flap, which can help suppress the clutter in the side flap direction. It should be noted that, although our method produces a lower side flap, the depression energy between the main flap and the side flap becomes higher, which is the inevitable result of weighting the frequency offsets with a window function. However, this does not affect the detection because the side flap energy is still low compared with the main flap, and the jamming signal inside the side flap can be easily found during the detection process by aligning the main flap to the detection target. The range-dimensional slicing of the beam map can better reflect the performance of the beam, and the comparison of each method is shown in Figure 6.

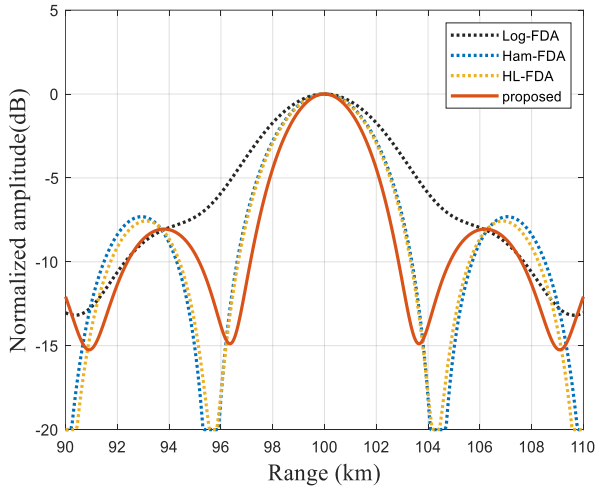


Figure 6. Range-Dimensional Slicing Performance Comparison.

As shown in Figure 6, the proposed scheme has greater advantages at both the main flap and the side flap because the Chebyshev window function is used to evenly disperse the energy in the side flap to the airspace far away from the main flap. Compared with several proposed methods, our proposed scheme has better beam-focusing performance with a narrower main flap and good side flap height, and the half-power beamwidth diagram can be a good comparison of the performance gap of the scheme, as shown in Figure 7.

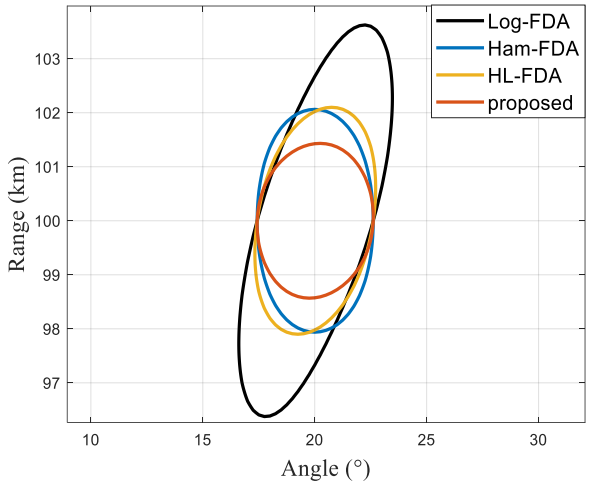


Figure 7. Half-power beamwidth diagram.

As represented in Figure 7, the half-power beamwidth comparison results show the superior performance of our proposed scheme in both angular and range dimensions.

5.2. Analysis of the Anti-Jamming Characteristics of the Proposed Scheme

In this section, we verify the anti-jamming capability of the proposed frequency offsets scheme in the presence of jamming in space and verify its beam performance under MVDR conditions, respectively. In the experiment, a range-dimensional jamming and an angle-dimensional jamming are set up, respectively. It can be seen that Jamming 1 is at the same angle as the target but at a different range; it is located on the side flap of the range dimension, and its beam gain is lower than the gain at the target point. Jamming 2 is at the same range from the target but at a different angle; it is located in the angular dimension of the side flap, and its gain is also lower than that at the target point. Meanwhile, we can see from the range slice and angle slice that after the adaptive beam formation, the beam of FDA-MIMO radar will automatically form a null trap at the jamming to suppress the jamming, but for the linear frequency offsets FDA-MIMO, it still has more energy distribution in the angle dimension, which indicates its weak anti-jamming capability in the angle dimension. The details are shown in Figure 8.

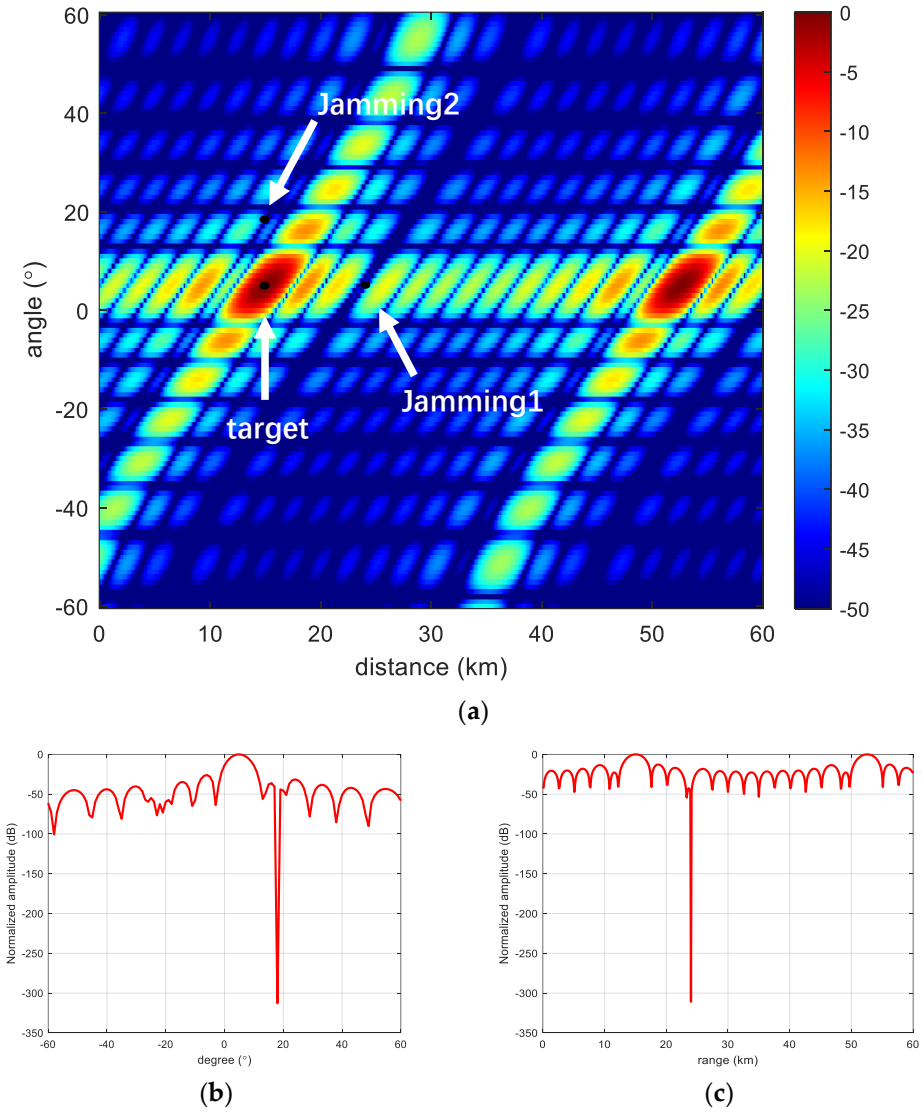
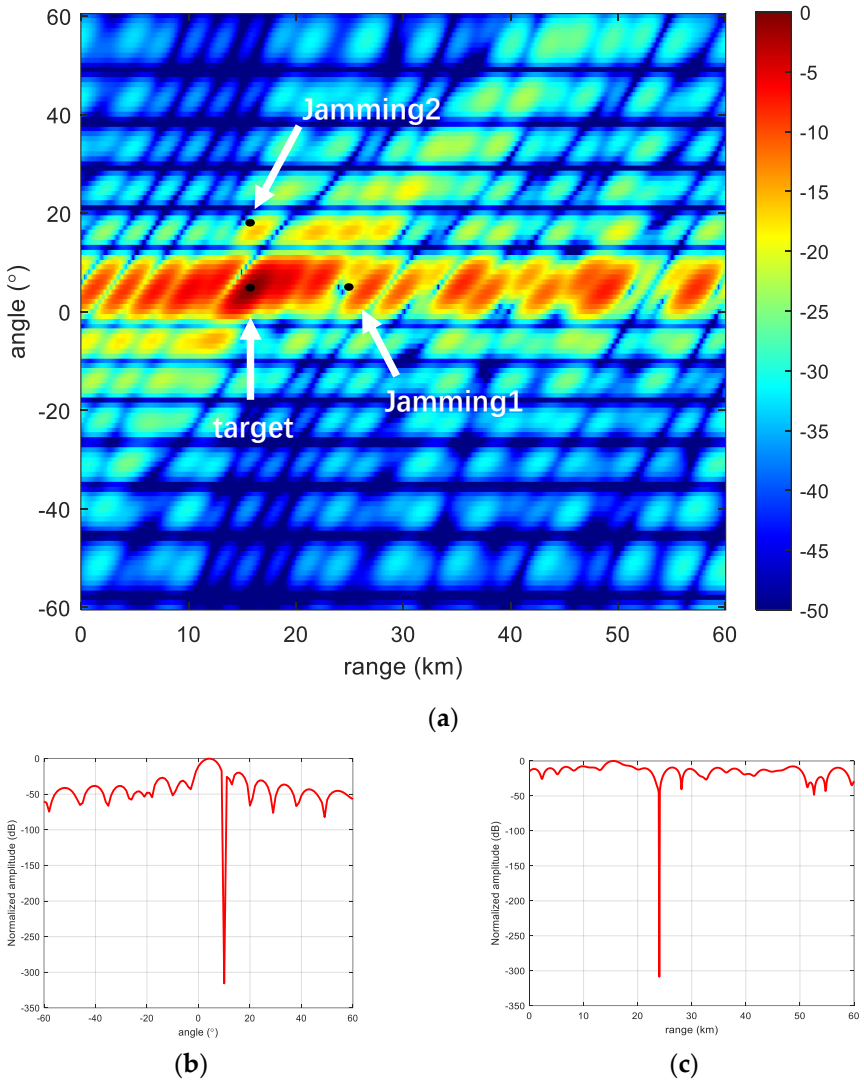


Figure 8. Linear frequency offset FDA-MIMO. (**a**) FDA-MIMO; (**b**) Range-dimensional slicing; and (**c**) Angle-dimensional slicing.

Figure 9 shows the beamforming performance of Log-FDA under MVDR conditions. It can be seen that the main flap of the Log-FDA beam becomes very wide and the position of the peak of the main flap is shifted, which indicates that Log-FDA does not adapt well to the environment where jamming is present.

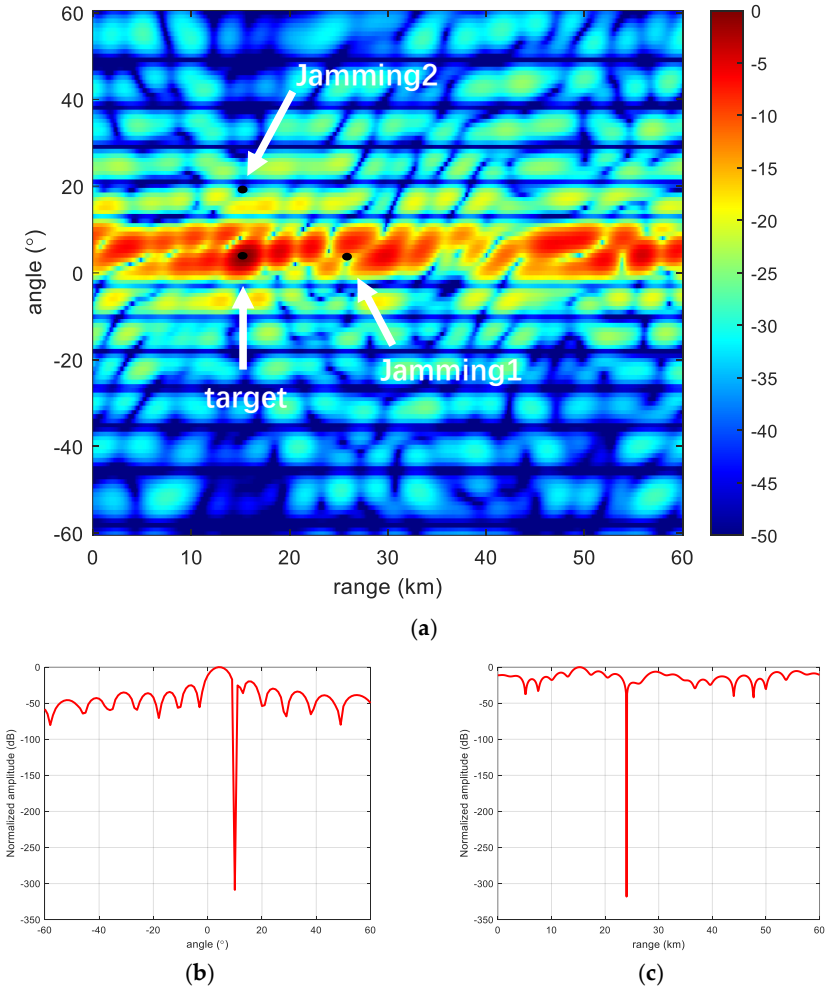


(**a**)

(**b**) (**c**)

Figure 9. Log-FDA performance. (**a**) Log-FDA; (**b**) Range-dimensional slicing; and (**c**) Angle-dimensional slicing.

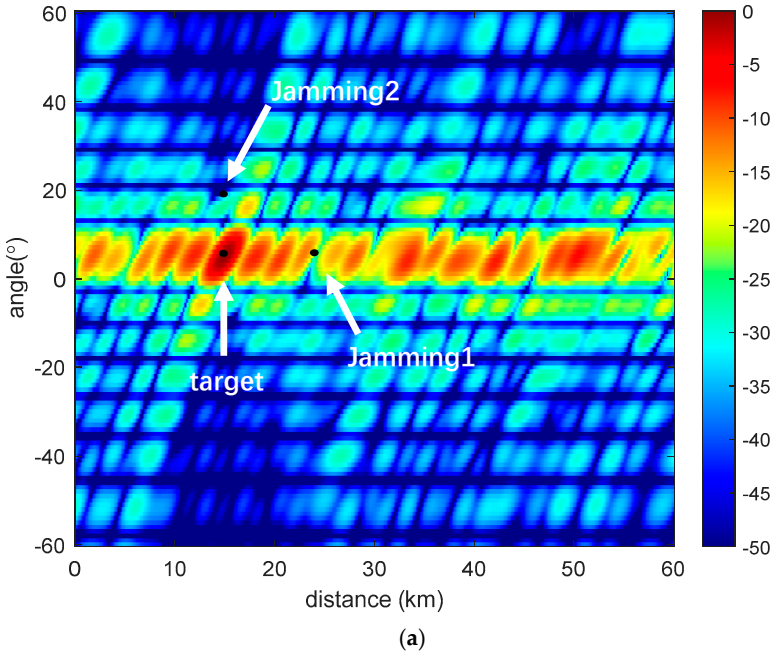
Figures 10 and 11 show the beamforming performance of HL-FDA under MVDR conditions. It can be seen that both HL-FDA and the proposed scheme can adapt well to the MVDR algorithm and can form zero traps at jamming locations in the presence of jamming in space. By observing the slice plots, it can be seen that the proposed scheme has a higher side flap in the range dimension but a narrower main flap width, which can better suppress jamming close to the main flap, which is one of the challenges faced by radar detection. Figure 12 shows the comparison of the output SINR in the presence and non-existence of MVDR conditions. It can be seen from the figure that the method in this paper has certain advantages over the traditional linear frequency bias method, which indicates that it is more applicable to the MVDR algorithm.



(**a**)

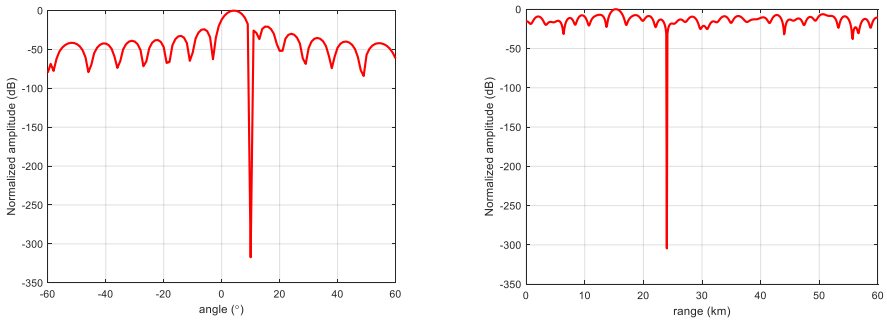
(**b**) (**c**)

Figure 10. HL-FDA performance. (**a**) HL-FDA; (**b**) Range-dimensional slicing; and (**c**) Angle-dimensional slicing.



(**a**)

Figure 11. *Cont.*



(**b**) (**c**)

Figure 11. Proposed scheme performance. (**a**) The proposed scheme; (**b**) Range-dimensional slicing; and (**c**) Angle-dimensional slicing.

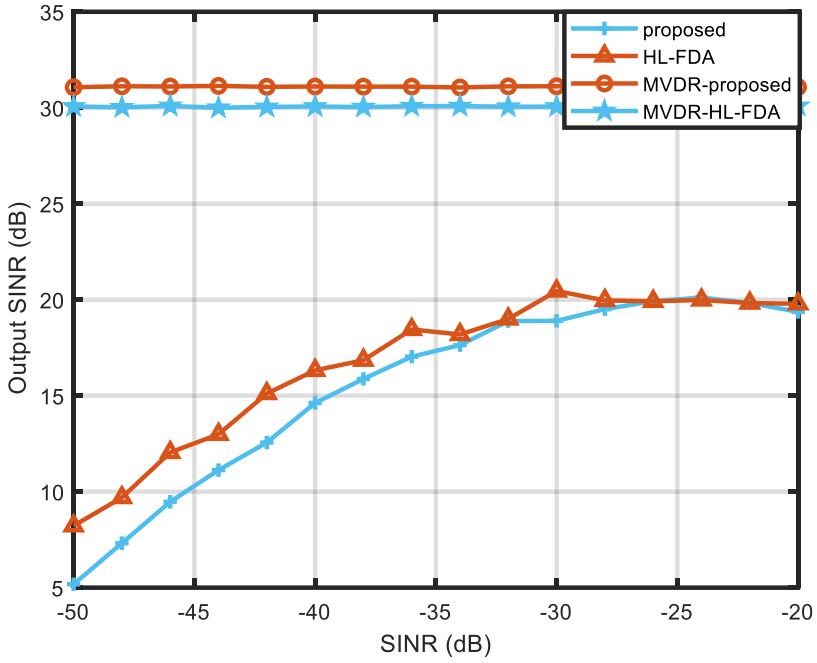


Figure 12. Comparison of output SINR.

6. Experimental Results and Discussion

In this paper, the coupling problem of FDA radar is solved using the FDA-MIMO system, a new nonlinear frequency offset scheme is proposed, and its anti-interference performance is verified relative to several other frequency offset schemes using the MVDR algorithm. Considering that most of the current studies focus on the optimization using fixed window function weighting, this paper utilizes the Chebyshev window function to optimize the FDA frequency offset for the first time. Compared with the currently proposed HL-FDA algorithm and Ham-FDA algorithm, the algorithm proposed in this paper has better performance with the correct selection of parameters and better anti-interference performance when there is interference in space. However, since this method requires the selection of parameters, it may require more computation time in practical applications.

Author Contributions: Methodology, G.Z. and M.T.; Writing—original draft, Y.X.; Supervision, C.W. All authors have read and agreed to the published version of the manuscript.

Funding: This work is supported by the National Natural Science Foundation of China (62201580); by Natural Science Foundation of Shaanxi (2021JM-222); by China Postdoctoral Science Foundation (2019M6622257).

Institutional Review Board Statement: Not applicable.

Informed Consent Statement: Not applicable.

Data Availability Statement: All data used in this paper can be obtained by contacting the authors of this study.

Conflicts of Interest: The authors declare no conflict of interest.

References

1. Antonik, P.; Wicks, M.C.; Griffiths, H.D.; Baker, C.J. Frequency diverse array radars. In Proceedings of the 2006 IEEE Conference on Radar, Verona, NY, USA, 24–27 April 2006; IEEE: Piscataway, NJ, USA, 2006; pp. 215–217.
2. Wang, W.-Q. Overview of frequency diverse array in radar and navigation applications. *IET Radar Sonar Navig.* **2016**, *6*, 1001–1012. [CrossRef]
3. So, H.C.; Amin, M.G.; Blunt, S.; Gini, F.; Wang, W.-Q. Introduction to the special issue on time-frequency modulated array signal processing. *IEEE J. Sel. Top. Signal Process.* **2020**, *2*, 225–227.
4. Xu, J.; Liao, G.; Zhu, S.; Huang, L.; So, H.C. Joint range and angle estimation using MIMO radar with frequency diverse array. *IEEE Trans. Signal Process.* **2015**, *13*, 3396–3410. [CrossRef]
5. Xu, J.; Zhu, S.; Liao, G.; Zhang, Y. An Overview of Frequency Diverse Array Radar Technology. *J. Radars* **2018**, *7*, 167–182.
6. Chen, H.; Wang, W.-Q.; Cui, Y.-S.; Liao, Y. Statistical analysis for time modulation-based frequency diverse array beam-pattern. *IEEE Access* **2019**, *7*, 84142–84154. [CrossRef]
7. Cheng, Q.; Zhu, J.; Xie, T.; Luo, J.; Xu, Z. Time-invariant angle-range dependent directional modulation based on time-modulated frequency diverse arrays. *IEEE Access* **2017**, *5*, 26279–26290. [CrossRef]
8. Xu, J.; Kang, J.; Liao, G.; So, H.C. Mainlobe deceptive jammer suppression with FDA-MIMO radar. In Proceedings of the 2018 IEEE 10th Sensor Array and Multichannel Signal Processing Workshop (SAM), Sheffield, UK, 8–11 July 2018; IEEE: Piscataway, NJ, USA; pp. 504–508.
9. Lan, L.; Liao, G.; Xu, J.; Zhang, Y.; Fioranelli, F. Suppression approach to main-beam deceptive jamming in FDA-MIMO radar using nonhomogeneous sample detection. *IEEE Access* **2018**, *6*, 34582–34597. [CrossRef]
10. Tan, M.; Wang, C.; Li, Z. Correction analysis of frequency diverse array radar about time. *IEEE Trans. Antennas Propag.* **2021**, *69*, 834–847. [CrossRef]
11. Xu, Y.; Shi, X.; Li, W.; Xu, J.; Huang, L. Low-sidelobe range-angle beamforming with FDA using multiple parameter optimization. *IEEE Trans. Aerosp. Electron. Syst.* **2019**, *55*, 2214–2225. [CrossRef]
12. Khan, W.; Qureshi, I.M.; Saeed, S. Frequency diverse array radar with logarithmically increasing frequency offset. *IEEE Antennas Wirel. Propag. Lett.* **2015**, *14*, 499–502. [CrossRef]
13. Xu, Y.; Xu, J. Corrections to range-angle-dependent beamforming of pulsed-frequency diverse array. *IEEE Trans. Antennas Propag.* **2018**, *66*, 6466–6468. [CrossRef]
14. Lan, L.; Liao, G.; Xu, J.; Wen, J. Range-angle pencil-beamforming for non-uniformly distributed array radar. *Multidimens. Syst. Signal Process.* **2018**, *29*, 867–886. [CrossRef]
15. Basit, A.; Qureshi, I.M.; Khan, W.; Rehman, S.U.; Khan, M.M. Beam Pattern Synthesis for an FDA Radar with Hamming Window-Based Nonuniform Frequency Offset. *IEEE Antennas Wirel. Propag. Lett.* **2017**, *16*, 2283–2286. [CrossRef]
16. Zhou, C.; Wang, C.; Gong, J.; Tan, M.; Zhao, Y.; Liu, M. FDA-MIMO Beampattern Synthesis with an Analytical Method. *Int. J. Aerosp. Eng.* **2021**, *2021*, 9051131. [CrossRef]
17. Tan, M.; Wang, C.; Yuan, H.; Bai, J.; An, L. FDA-MIMO Beampattern Synthesis with Hamming Window Weighted Linear Frequency Increments. *Int. J. Aerosp. Eng.* **2020**, *2020*, 4851909. [CrossRef]
18. Basit, A.; Wang, W.; Nusenu, S. Adaptive transmit array sidelobe control using FDA-MIMO for tracking in joint radar-communications. *Digit. Signal Process.* **2020**, *97*, 102619. [CrossRef]
19. Lan, L.; Liao, G.; Xu, J.; Zhu, S.; Zhang, Y. Range-angle-dependent beamforming for FDA-MIMO radar using oblique projection. *Sci. China Inf. Sci.* **2022**, *65*, 152305. [CrossRef]
20. Lan, L.; Liao, G.; Xu, J.; Zhang, Y.; Liao, B. Transceive Beamforming With Accurate Nulling in FDA-MIMO Radar for Imaging. *IEEE Trans. Geosci. Remote Sens.* **2020**, *58*, 4145–4159. [CrossRef]
21. Wen, F.; Gui, G.; Gacanin, H.; Sari, H. Compressive sampling framework for 2D-DOA and polarization estimation in mmWave polarized massive MIMO systems. *IEEE Trans. Wirel. Commun.* **2022**. [CrossRef]
22. Wen, F.; Shi, J.; Gui, G. 3D Positioning method for anonymous UAV based on bistatic polarized MIMO radar. *IEEE Internet Things J.* **2023**, *10*, 815–827. [CrossRef]
23. Liao, Y.; Tang, H.; Chen, X.; Wang, W.-Q. Frequency Diverse Array Beampattern Synthesis With Taylor Windowed Frequency Offsets. *IEEE Antennas Wirel. Propag. Lett.* **2020**, *19*, 1901–1905. [CrossRef]
24. Sun, Z.; Huang, J.; Yang, J.; Zang, T.; He, Z. A High Accuracy Analysis Method of Harmonic/Interharmonic in Power System Based on Chebyshev Window. *Autom. Electr. Power Syst.* **2015**, *39*, 117–123.

Disclaimer/Publisher's Note: The statements, opinions and data contained in all publications are solely those of the individual author(s) and contributor(s) and not of MDPI and/or the editor(s). MDPI and/or the editor(s) disclaim responsibility for any injury to people or property resulting from any ideas, methods, instructions or products referred to in the content.